

# Osteoblast-Targeted suppression of PPAR increases osteogenesis through activation of mTOR signaling

Hongli Sun, Jin Koo Kim, Richard Mortensen, Lorraine P. Mutyaba, Kurt D. Hankenson, Paul H. Krebsbach



The advertisement banner features a dark blue background on the left with a white control panel on a piece of equipment. The text is arranged in three lines: the top line in green, the middle line in white, and the bottom line in white on a green background. The PHCbi logo is on the right.

You Don't Need Reproducible Research  
**UNTIL YOU DO.**  
Minimize uncertainty with PHCbi brand products

**phcbi**

## Osteoblast-Targeted Suppression of PPAR $\gamma$ Increases Osteogenesis Through Activation of mTOR Signaling

HONGLI SUN,<sup>a</sup> JIN KOO KIM,<sup>a</sup> RICHARD MORTENSEN,<sup>b</sup> LORRAINE P. MUTYABA,<sup>c</sup> KURT D. HANKENSON,<sup>c</sup> PAUL H. KREBSBACH<sup>a\*</sup>

<sup>a</sup>Department of Biologic and Materials Sciences, University of Michigan School of Dentistry, Ann Arbor, Michigan, USA; <sup>b</sup>Department of Physiology, University of Michigan School of Medicine, Ann Arbor, Michigan, USA;

<sup>c</sup>Department of Clinical Studies-New Bolton Center, School of Veterinary Medicine and Department of Orthopaedic Surgery, Perelman School of Medicine, University of Pennsylvania, Philadelphia, Pennsylvania, USA

**Key words:** Fat • Bone • mTOR • PPAR $\gamma$ ; RUNX2 • Osteoblast

### ABSTRACT

Nuclear receptor peroxisome proliferator-activated receptor- $\gamma$  (PPAR $\gamma$ ) is an essential transcription factor for adipocyte differentiation. In mesenchymal stem cells, PPAR $\gamma$  has been assumed to play a negative role in osteoblastic differentiation, by working in an adipogenesis dependent manner, due to the reciprocal relationship between osteoblast and adipocyte differentiation. However, the direct role of PPAR $\gamma$  in osteoblast function is not fully understood, due in part to inadequate model systems. Here, we describe an adenoviral-mediated PPAR $\gamma$  knockout system in which suppression of PPAR $\gamma$  in mesenchymal stem cells enhanced osteoblast differentiation and inhibited adipogenesis *in vitro*. Consistent with this *in vitro* observation, lipotrophic A-ZIP/F1 mice, which do not form adipocytes, displayed a phenotype in which both cortical and trabecular bone was significantly increased compared with wild-

type mice. We next developed an inducible osteoblast-targeted PPAR $\gamma$  knockout (*Osx Cre/flox-PPAR $\gamma$* ) mouse to determine the direct role of PPAR $\gamma$  in bone formation. Data from both *in vitro* cultures of mesenchymal stem cells and *in vivo*  $\mu$ CT analysis of bones suggest that suppression of PPAR $\gamma$  activity in osteoblasts significantly increased osteoblast differentiation and trabecular number. Endogenous PPAR $\gamma$  in mesenchymal stem cells and osteoblasts strongly inhibited Akt/mammalian target of rapamycin (mTOR)/p70S6k activity and led to decreased osteoblastic differentiation. Therefore, we conclude that PPAR $\gamma$  modulates osteoblast differentiation and bone formation through both direct and indirect mechanisms. The direct mode, as shown here, involves PPAR $\gamma$  regulation of the mTOR pathway, while the indirect pathway is dependent on the regulation of adipogenesis. *STEM CELLS* 2013;31:2183–2192

Disclosure of potential conflicts of interest is found at the end of this article.

### INTRODUCTION

Nuclear receptor peroxisome proliferator-activated receptor- $\gamma$  (PPAR $\gamma$ ) is an essential transcription factor for adipocyte differentiation. Evidence for this requirement is derived from observations that embryonic stem cells (ESC) from mice lacking PPAR $\gamma$  are unable to differentiate into fat tissue [1] and that over-expression of PPAR $\gamma$  in fibroblasts initiates adipogenesis [2]. Expression of PPAR $\gamma$  is activated by naturally occurring fatty acids, peroxisome proliferators, and the thiazolidinedione (TZD) class of antidiabetic agents [3]. The TZDs, which function to lower blood glucose, have been widely used for the treatment of type 2 diabetes mellitus. Unfortunately, a significant side effect of this therapy is the potential for bone loss and subsequent skeletal fractures in diabetic

patients [4]. This clinical consequence may be due to an imbalance between osteogenesis and adipogenesis when PPAR $\gamma$  is overactivated in response to TZD [4]. However, the specific role of PPAR $\gamma$  in osteogenesis is not fully understood.

A direct role for PPAR $\gamma$  in bone formation has been difficult to determine because of the reciprocal regulation relationship that is hypothesized to exist between osteoblast and adipocyte differentiation of mesenchymal progenitor cells. For example, age-related osteoporosis is most often accompanied by an increase in bone marrow adipose tissue and it is believed that fat increases when osteoblasts are decreased because progenitors form adipocytes instead of osteoblasts [5]. In contrast, PPAR $\gamma$ -deficient ES cells fail to differentiate into adipocytes, but instead spontaneously differentiate into osteoblasts [1]. In transgenic animal models, PPAR $\gamma$ -

Author contributions: H.S.: conception and design, collection and/or assembly of data, data analysis and interpretation, manuscript writing, and final approval of manuscript; J.K.K.: collection and/or assembly of data, data analysis and interpretation, manuscript writing, and final approval of manuscript; R.M.M. and P.L.M.: provision of study material, collection and/or assembly of data, data analysis and interpretation, and final approval of manuscript; K.D.H.: conception and design, financial support, data analysis and interpretation, and final approval of manuscript; P.H.K.: conception and design, financial support, data analysis and interpretation, manuscript writing and final approval of manuscript.

Correspondence: Paul H. Krebsbach, D.D.S., Ph.D., Department of Biologic and Materials Sciences, School of Dentistry, University of Michigan, 1011 North University Ave, Ann Arbor, Michigan 48109, USA. Telephone: +734-936-2600; Fax: +734-647-2110; e-mail: paulk@umich.edu. Received December 12, 2012; accepted for publication May 21, 2013; first published online in *STEM CELLS EXPRESS* June 14, 2013. © AlphaMed Press 1066-5099/2013/\$30.00/0 doi: 10.1002/stem.1455

insufficient mice exhibit high bone mass with increased osteogenesis and decreased adipogenesis [6]. Adipocytes also directly modulate osteoblast function through paracrine effects of secretory adipocytokines, such as adiponectin and leptin [7–10]. Taken together, these data suggest that PPAR $\gamma$  regulates bone formation in an indirect manner, a reciprocal effect of its primary modulation of adipogenesis and/or through adipocytokines. However, functional PPAR $\gamma$  is also expressed in mouse and human osteoblasts [11–13], which suggests that PPAR $\gamma$  may play a direct role in regulating osteogenesis. One recent study indicates that osteoblast-targeted over-expression of PPAR $\gamma$  significantly reduces bone mass in mice [14]. However, it has also been reported that over-expression of PPAR $\gamma$  induces trans-differentiation of osteoblasts to adipocytes [15]. The PPAR $\gamma$  over-expression mouse model is therefore not sufficient to completely understand the physiologic role of PPAR $\gamma$  in osteogenesis. Moreover, recent evidence indicates that suppression of adipogenesis by inhibition of PPAR $\gamma$  is not able to increase osteogenesis either in vitro or in vivo [16,17]. Therefore, it is essential to determine the extent to which PPAR $\gamma$  has a direct role in osteoblast function and bone formation.

Because the molecular mechanisms by which PPAR $\gamma$  could regulate osteoblasts are not fully understood, we sought to determine how PPAR $\gamma$  might interact with a key metabolic signaling pathway in bone. Mammalian target of rapamycin (mTOR) is the catalytic subunit of two distinct signaling complexes, mTOR complexes 1 and 2 (mTORC1 and mTORC2) [18]. mTORC1 activates ribosomal S6 kinase (S6K) and inactivates eukaryotic initiation factor 4E binding protein 1 (4EBP1) and thus stimulates protein synthesis, cell growth, cell proliferation, and progression through the cell cycle. Promotion of cell survival and cytoskeletal reorganization is also enhanced when mTORC2 activates Akt and PKC $\alpha$  [19–21]. Recent work also supports an important role of mTOR in the regulation of cell differentiation [22–25].

It is well known that the global protein translation level in stem cells is lower than differentiated cells, whereas the activation of protein translation in these stem cells can initiate differentiation [22–25]. We, and others, recently demonstrated that mTOR signaling plays an essential role in osteoblast differentiation in vitro [26–30]. It is notable that rapamycin, an inhibitor of mTOR, inhibits osteogenesis both in vitro and in vivo [31]. Moreover, mTOR also plays an important role in PPAR $\gamma$ -mediated adipogenesis [32,33]. These data suggest a potential for crosstalk between the mTOR and PPAR $\gamma$  pathways, both of which are important for osteogenesis. In this study, we used in vitro models and developed a new osteoblast-specific PPAR $\gamma$  knockout mouse to study the physiologic role of endogenous PPAR $\gamma$  in bone formation and found that the mTOR pathway was directly involved in PPAR $\gamma$ -mediated modulation of osteogenesis and conclude that PPAR $\gamma$  modulates bone formation through both direct and indirect mechanisms.

## MATERIALS AND METHODS

### Cell Culture

Bone marrow mesenchymal stem cells (BMSCs) were harvested and cultured as described previously [34,35] with modifications. Briefly, femora and tibiae were dissected free of surrounding soft tissues. The aspirates were flushed with  $\alpha$ -Modified Eagle's Medium ( $\alpha$ -MEM; Invitrogen, Carlsbad, CA), and filtered through a 40- $\mu$ m cell strainer. The marrow content of 4–6 bones was plated into a T75 culture flask in BMSC growth medium

comprised of  $\alpha$ -MEM containing 10% fetal bovine serum (FBS), 100 U/mL penicillin, 100 mg/mL streptomycin sulfate (Gibco, Grand Island, NY). Nonadherent cells were removed and adherent BMSCs were cultured and expanded for further experiments. Primary cells prior to passage four were used in the experiments. It is generally believed that BMSCs are the common progenitors for osteoblasts and adipocytes. As a primary cell type, BMSCs may more likely reflect the nature of cells of the bone marrow, in addition to their potential for clinical use when compared with cell lines. However, BMSCs are a heterogeneous population. Therefore, the well-defined bone marrow stromal cell line, ST2 [36], which has osteoblast/adipocyte bipotential, is an ideal cell type for mechanistic studies on the reciprocal relationship between osteoblast and adipocyte differentiation. Similarly, the preosteoblast cell line MC3T3-E1 is an appropriate cell type to study molecular mechanisms when the cells have been committed to osteoblasts. ST2 and MC3T3-E1 cells were cultured in High Glucose Dulbecco's Modified Eagle Medium (HG-DMEM) containing 10% FBS, 100U/mL penicillin, 100 mg/mL streptomycin sulfate (Gibco, Grand Island, NY), and  $\alpha$ -MEM containing 10% FBS, 100U/mL penicillin, and 100 mg/mL streptomycin sulfate, respectively.

PPAR $\gamma$  was activated by 5  $\mu$ g/mL Troglitazone (Trog, Cayman Chemical, Ann Arbor, MI), and the vehicle, dimethyl sulfoxide (DMSO, Sigma, St. Louis, MO.)-treated group was included as the control. BMSCs from PPAR $\gamma$  flox/flox mice were transfected with adenovirus as described previously [9] with minor modifications. The cells were plated at a density of 20,000 cells/cm<sup>2</sup> in T75 flasks. After 4 hours, virus was added at a multiplicity of infection of 1,000 in 4 mL  $\alpha$ -MEM with 0.5% FBS. The virus-containing medium was removed and complete fresh medium was added after 4-hour cell transduction. Adenovirus-expressing cre recombinase (Ad-Cre) was harvested on February 19, 2009, and viral titer was 2.40E11 plaque forming unit (PFU) per milliliter. Adenovirus CMVpLpA.dIE3 #1 (Ad-Blank) was harvested on February 18, 2001, and viral titer was 1.30E11 PFU per milliliter.

### Gene Expression Analysis

Polymerase chain reaction (PCR) analysis to detect knockout of PPAR $\gamma$  by Ad-Cre was performed as described previously [37] with modifications. Genomic DNA in the transfected BMSCs was harvested using the DNeasy Blood and Tissue Kit (Qiagen, Germantow, MD). The primers for genotyping included one forward primer 2F: CTC CAA TGT TCT CAA ACT TAC and two reverse primers 1R: GAT GAG TCA TGT AAG TTG ACC and H5: GTA TTC TAT GGC TTC CAG TGC. Primer pair 2F/1R was designed to amplify the intact PPAR $\gamma$  gene and the amplified length was 285 bp. Primer pair 2F/H5 was used to detect the deleted gene and the amplified length was 450 bp. Thermal cycling conditions were as follows: 95°C, 5 minutes, 40 cycles at (95°C, 30 seconds, 55°C, 30 seconds, 72°C, 45 seconds), 72°C, 5 minutes and 4°C. A 2% agarose-TAE gel electrophoresis followed by ethidium bromide staining was used to detect bands.

For the osteogenic and adipogenic gene expressions of the Ad-Cre BMSCs, the total RNA was isolated using the RNeasyMicro Kit (Qiagen, Germantow, MD). RNA concentration was determined at 260 nm and an equivalent amount of RNA sample (2  $\mu$ g) was processed to generate cDNA using the High Capacity cDNA Reverse Transcript kit (Applied Biosystems, Foster City, CA). Quantitative PCR was performed by the SYBR Green PCR method using the ABI PRISM 7,500 sequence detection system (Applied Biosystems, Carlsbad, CA, USA). The housekeeping gene glyceraldehyde 3-phosphate dehydrogenase (*GAPDH*) was used for normalization, *GAPDH* *F*: TGA AGC AGG CAT CTG AGG G; *GAPDH* *R*: CGA AGG TGG AAG AGT GGG AG. Primers for osteocalcin (*OCN*) and fatty acid binding protein 4 (*FABP4*) were: *OCN* *F*: CAA GCA GGG TTA AGC TCA CA; *OCN* *R*: GGT AGT GAA CAG ACT CCG GC [9]; *FABP4* *F*: AAT GTG TGA TGC CTT TGT GG; *FABP4* *R*: CAC TTT

CCT TGT GGC AAA GC. Gene expressions in ST2 and MC3T3-E1 cells were performed with Taqman gene expression assays (Applied Biosystems, Forster City, CA). The genes analyzed were: *GAPDH* (Mm99999915), *Runx2* (Mm00501584), *OCN* (Mm-03413826), and *PPAR $\gamma$*  (Mm01184322) (Applied Biosystems, Forster City, CA).

### In Vitro Mineralization Assays

The mineralization assay used for primary BMSCs was described previously [9]. Briefly, cells were plated in 12-well or 24-well plates at 20,000 cells/cm<sup>2</sup>. Plated cells were allowed to grow to confluence in growth medium. After reaching confluence, cells were cultured in osteogenic medium (BMSC Growth Medium + 100 nM dexamethasone, 10 mM  $\beta$ -glycerophosphate, and 50  $\mu$ M ascorbic acid 2-phosphate (all from Sigma, St. Louis, MO.)) for up to 14 days. The same protocol was used for ST2 and MC3T3-E1 cells except the osteogenic medium did not contain dexamethasone. Subsequently, cells were fixed with cold 70% ethanol for 1 hour, rinsed with water, stained for 10 minutes in 40 mM Alizarin red S (pH 4.2), and washed extensively with water. After imaging, the dye was eluted with 10% w/v hexadecylpyridinium chloride monohydrate (Wako, Chemical, Osaka, Japan) in 10 mM sodium phosphate pH 7.0 and concentration was determined by absorbance measurement at 562 nm. The results were normalized to total genomic DNA content.

### In Vitro Adipogenic Differentiation Assays

The adipogenic differentiation assay was performed as described previously [9]. Briefly cells were plated at 40,000 cells per square centimeter and grown to confluence in HG-DMEM growth medium (HG-DMEM containing 10% FBS, 100U/mL penicillin, and 100 mg/mL streptomycin sulfate). Cells were induced with adipogenic medium (HG-DMEM growth medium + 50  $\mu$ M isobutylmethylxanthine (Sigma, St. Louis, MO.), 1  $\mu$ M dexamethasone (Sigma, St. Louis, MO.), 167 nM insulin (Sigma, St. Louis, MO.), and 5  $\mu$ g/mL Troglitazone (Cayman Chemical, Ann Arbor, MI) for 2 days. Adipogenic maintenance medium (HG-DMEM Growth Medium + 167 nM insulin) was then added for another 2 days. This process of induction medium followed by maintenance media was repeated three times. Cells were then fixed in zinc-buffered formalin (Z-fix, Anatech LTD, Battle Creek, MI) for half hour and stained with oil red O solution (Sigma, St. Louis, MO.). Dye was eluted in 100% isopropanol and quantified at 500 nm. The results were normalized to total genomic DNA.

### Genetically Modified Mice

Animal experiments were approved by the institutional animal care and use committee. *PPAR $\gamma$* -floxed mice [19] were crossed with tetracycline regulatable osterix-Cre mice [38] purchased from Jackson Laboratories (B6.Cg-Tg(Sp7-tTA,tetO-EGFP/cre)1Amc/J; Stock Number: 006361). Mice were maintained on Doxycycline feed (Harlan Item #: TD.01306; Rodent Diet (2018, 625 Doxycycline) throughout the entire process of crossing the two lines to achieve homozygosity of the floxed *PPAR $\gamma$*  allele. Mice that were *Osx*-Cre positive/*PPAR $\gamma$*  f/f (experimental) or that were *Osx*-Cre negative/*PPAR $\gamma$*  f/f or (control) were removed from the Doxycycline feed at weaning (~3 weeks) and harvested at 6 months of age. For the in vitro experiments, BMSCs from the experimental and control mice were isolated, cultured and differentiated using the same methods as aforementioned. To further investigate the role of adipogenesis in bone formation in an in vivo context, we tested our hypothesis in A-ZIP/F1 fatless mice that do not form adipocytes due to the expression of a dominant-negative form of C/EBP under the *FABP4* promoter [39]. AZip-F1 mice were provided by Dr. Chuck Vinson and harvested as indicated for evaluation of bone geometric parameters using microCT.

### $\mu$ CT 3D Reconstruction and Bone Morphometry

Femurs were fixed for 2 days with Z-fix (Anatech LTD, Battle Creek, MI), then moved to 70% ethanol, and scanned at a voxel

size of 18  $\mu$ m using a  $\mu$ CT scanner (GE Healthcare Pre-Clinical Imaging, London, ON). Micro View software (GE Healthcare Pre-Clinical Imaging) was used to generate a three-dimensional reconstruction from the set of scans. Assessment of bone microstructure was carried out according to the guidelines developed by Bouxsein et al. [40]. The region selected for cortical bone parameters was defined to be the central portion between the proximal and distal ends of the femur. Trabecular bone parameters were measured by analyzing the metaphyseal region adjacent to growth plate. User-defined contours were drawn every five images and interpolated for all images in between. The thresholds for cortical and trabecular bone were set to 2,000 and 1,200, respectively.

### Western Blot Analysis

Primary BMSCs transfected with Ad-Cre/Ad-Blank after 3 days were harvested for Western Blot analysis. ST2 and MC3T3-E1 cells were treated with 50  $\mu$ M bisphenol A diglycidyl ether (BADGE, Sigma, St. Louis, MO.) for 24 hours and harvested as well for Western Blot analysis as described previously [26]. Briefly, whole cell lysates were separated on 10% SDS-polyacrylamide gel and transferred to PVDF membrane. The membranes were incubated with 5% milk for 1 hour and incubated with primary antibodies overnight at 4°C. Primary antibodies used were as follows: polyclonal anti-phospho-AKT (1:500; Cell Signaling, Danvers, MA), polyclonal anti-AKT (1:1,000; Cell Signaling), polyclonal anti-phospho-p70S6K (1:500; Cell Signaling), polyclonal anti-p70S6K (1:1,000; Cell Signaling), polyclonal anti-PPAR $\gamma$  (1:1,000; Santa Cruz Biotechnology, Santa Cruz, CA), polyclonal anti-RUNX2 (1:1,000; Santa Cruz), and polyclonal anti-Osteocalcin (1:1,000; Millipore). Blots were incubated with peroxidase-coupled secondary antibodies (Promega, Madison, WI) for 1 hour, and protein expression was detected with SuperSignal West Pico Chemiluminescent Substrate (Thermo Scientific, Rockford, IL). Membranes were reprobbed with polyclonal anti- $\beta$ -actin antibody (1:1,000; Cell Signaling) to control for equal loading.

### Statistical Analysis and Image Editing

To determine statistical significance of observed differences between the study groups, a two-tailed homoscedastic *t*-test was applied. A value of  $p < .05$  was considered to be statistically significant while  $0.05 < p < .10$  was considered to represent a non-significant, but clear trend in cell or tissue response. Values are reported as the mean  $\pm$  SD. Brightness and contrast were adjusted equally across all images for improved visibility.

## RESULTS

### Knockout of *PPAR $\gamma$* in BMSCs Increases Osteogenesis and Inhibits Adipogenesis

Primary BMSCs were isolated from *PPAR $\gamma$*  flox/flox mice to study the effects of *PPAR $\gamma$*  gene knockout on adipogenesis and osteogenesis. PCR-based genotyping assays demonstrated robust *LoxP* recombination indicating loss of *PPAR $\gamma$*  at the gene level (450bp band) in BMSCs after Ad-Cre delivery, while no band was detected in the control group (Ad-Blank) (Fig. 1A). It was noted that residual intact *PPAR $\gamma$*  (285 bp band) remained in the deleted group. Consistent with the essential role of *PPAR $\gamma$*  in adipogenesis, the adipogenic differentiation of BMSCs was largely inhibited by in vitro *PPAR $\gamma$*  gene knockout. When *PPAR $\gamma$*  expression was abrogated, oil red O staining and *FABP4* gene expression was diminished (Fig. 1B). In contrast, *PPAR $\gamma$*  knockout led to significantly increased mineralization and *OCN* gene expression in BMSCs (Fig. 1C). This in vitro adenoviral-mediated *PPAR $\gamma$*  knockout system therefore demonstrated that

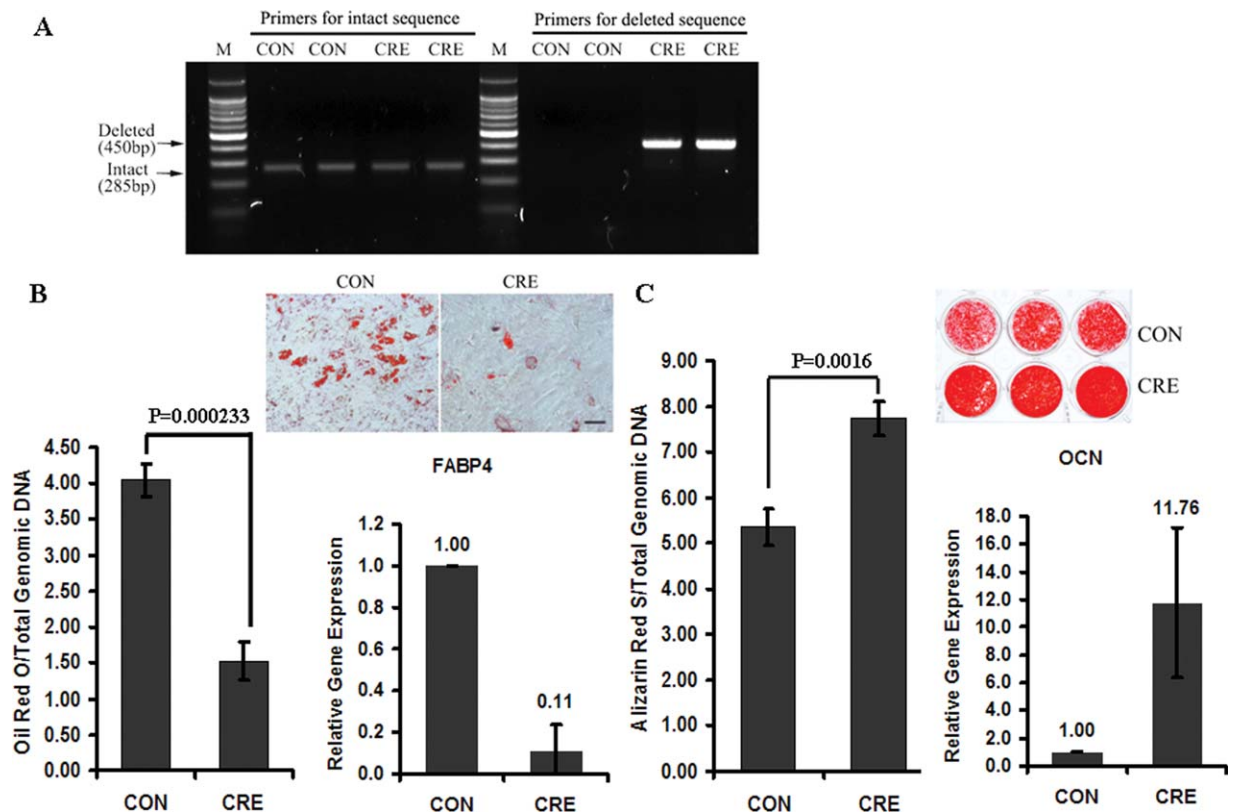


**Figure 1.** Knockout of *PPAR $\gamma$*  in bone marrow mesenchymal stem cells (BMSCs) increases osteogenesis and inhibits adipogenesis. (A): Polymerase chain reaction-based genotyping. The deleted bands (450 bp) were detected only in the AdCRE group (CRE), while the intact bands (285 bp) were detected in both control (CON) and CRE groups. (B): *PPAR $\gamma$*  is essential for adipogenesis in BMSCs. Oil red O staining and *FABP4* gene expression were diminished when *PPAR $\gamma$*  expression was abrogated by Ad-Cre ( $n = 3$ ). (C): *PPAR $\gamma$*  knockout increases osteogenesis. *PPAR $\gamma$*  knockout led to significantly increased mineralization and *OCN* gene expression in BMSCs ( $n = 3$ ). Data are expressed as means  $\pm$  SD. Scale bar = 50  $\mu$ m. Abbreviations: CON, control; CRE, AdCRE group; *FABP4*, fatty acid binding protein 4.

suppression of *PPAR $\gamma$*  enhanced osteogenesis and reduced adipogenesis.

### Osteogenesis Is Modulated by PPAR $\gamma$ -Mediated Adipogenesis In Vitro and In Vivo

After a 2-week culture period in osteogenic medium, ST2 cells were strongly positive for Alizarin red S staining (Fig. 2A). This finding is in contrast to the effects observed when *PPAR $\gamma$*  was activated. Mineralization of ST2 cells was inhibited when *PPAR $\gamma$*  was activated by troglitazone, a *PPAR $\gamma$*  ligand that supports *PPAR* activation. Accordingly, troglitazone-treated ST2 cells switched to an adipogenic phenotype with oil red O-positive lipid droplets accumulating in cultured cells (Fig. 2A), suggesting that osteogenesis was negatively modulated by *PPAR $\gamma$* -induced adipogenesis.

Micro-CT data from A-ZIP/F1 mouse long bones demonstrated a clear trend ( $0.05 < p < .10$ ) in which cortical bone was increased in A-ZIP/F1 relative to wild-type mice. These parameters included mean cortical thickness, bone mineral content (BMC) and bone mineral density (BMD). In line with this trend, the marrow area in A-ZIP/F1 bones was significantly lower than in wild-type mice (Fig. 2B). Compared with cortical bone, the effects of adipogenic deficiency were more profound for trabecular bone formation in A-ZIP/F1 mice. The bone  $\mu$ CT values, including bone surface/bone volume (BS/BV) and trabecular spacing (Tb.Sp.), were significantly decreased, while trabecular number (Tb.N) was significantly increased in A-ZIP/F1 mice. The bone/tissue volume (BV/TV) ratio also indicated a higher trend ( $0.05 < p < .10$ ) in A-ZIP/F1 mice (Fig. 2C). Therefore,

both our in vitro and in vivo data indicated that *PPAR $\gamma$* -mediated adipogenesis negatively regulated bone formation.

### Osteoblast-Targeted PPAR $\gamma$ Suppression Increased Osteogenesis In Vitro

Based on the opposing effects on mineralization when *PPAR $\gamma$*  was either knocked out or activated, we hypothesized that the inhibitory effects of *PPAR* activation on bone formation were due, in part, to its proadipogenic function. Therefore, to determine if *PPAR $\gamma$*  had a direct role in osteogenesis that was independent on adipogenesis, BMSCs from osteoblast-targeted *PPAR $\gamma$*  knockout mice were isolated and their capacity for osteogenic differentiation was examined. Compared with the BMSCs from WT mice, BMSCs from osteoblast-targeted *PPAR $\gamma$*  knockout mice demonstrated much higher mineralization after 2 weeks in culture in osteogenic differentiation medium (Fig. 3A). The finding that mineralization was enhanced when *PPAR $\gamma$*  was blocked was corroborated in pre-osteoblastic MC3T3-E1 cells when they were treated with BADGE, an effective antagonist of *PPAR $\gamma$*  (Fig. 3B). The effects of *PPAR $\gamma$*  inhibition on osteoblast-related gene expression in ST2 and MC3T3-E1 were tested after 24 hours BADGE treatment. *Osteocalcin* gene expression was enhanced by BADGE, while no significant difference was noticed for *Runx2* expression in either cell type. Interestingly, expression of *PPAR $\gamma$*  was also increased by BADGE treatment (Fig. 3C). Taken together, these data suggest that *PPAR $\gamma$*  in osteoblasts or preosteoblastic cells is able to modulate osteogenic differentiation through a direct manner in vitro.

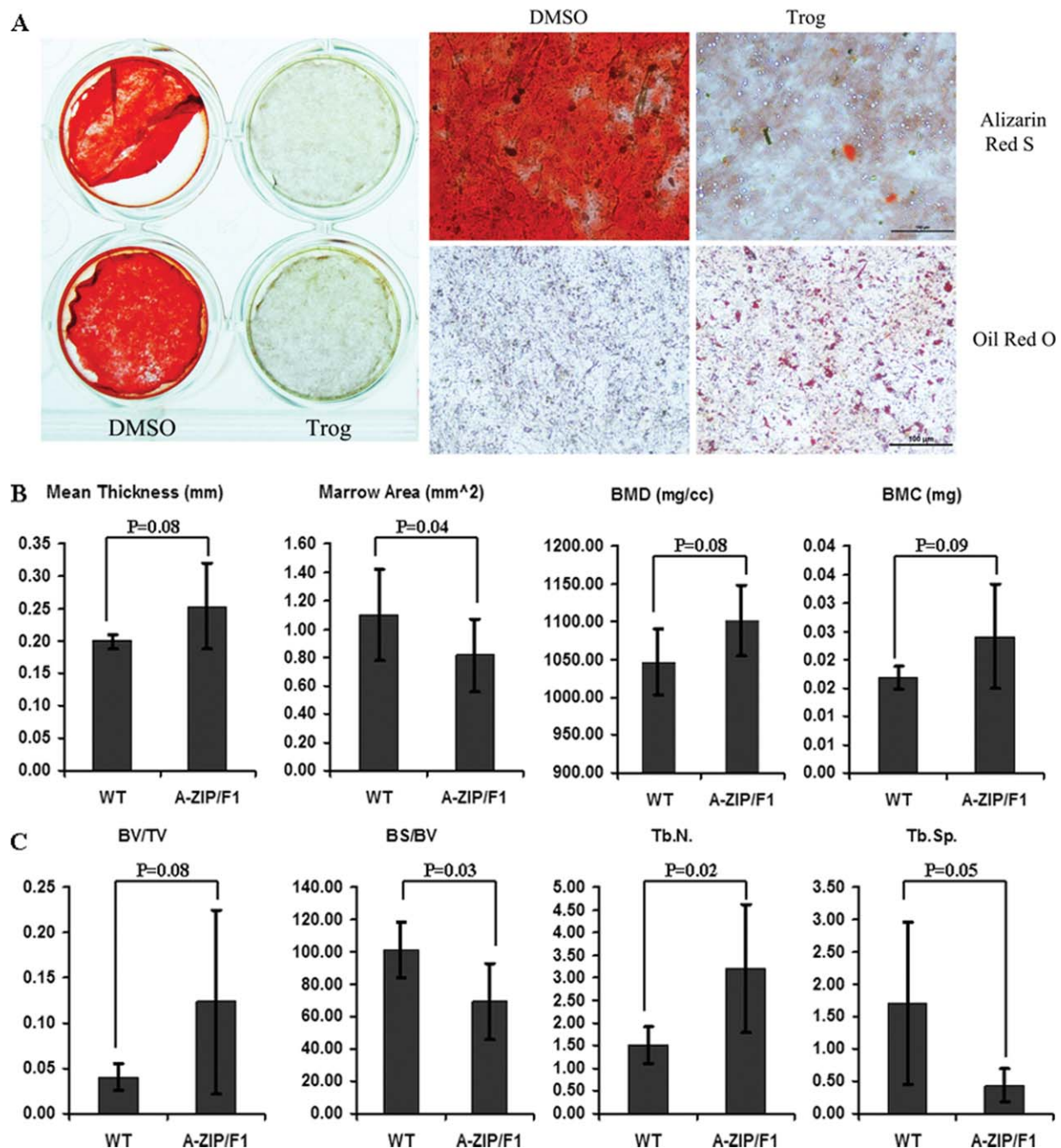


**Figure 2.** Osteogenesis is modulated by PPAR $\gamma$ -mediated adipogenesis in vitro and in vivo. (A): Osteogenic differentiation of ST2 cells is inhibited by PPAR $\gamma$  activation. After a 2-week culture in osteogenic medium, ST2 cells were strongly positive for alizarin red S staining. Mineralization of ST2 cells was inhibited when PPAR $\gamma$  was activated by troglitazone. Accordingly, troglitazone-treated ST2 cells switched to an adipogenic phenotype with oil red O-positive lipid droplets in cultured cells ( $n = 4$ ). Scale bar = 100  $\mu$ m. (B): Cortical bone formation is increased in A-ZIP/F1 fatless mice. Micro-CT data, including mean cortical thickness, bone mineral content (BMC), and bone mineral density (BMD), demonstrated a clear trend ( $0.05 < p < .10$ ) that cortical bone was increased in A-ZIP/F1 ( $n = 5$ ) relative to wild-type ( $n = 6$ ) mice. The marrow area in A-ZIP/F1 bones was significantly lower than in wild-type mice. (C): Trabecular bone formation is increased in A-ZIP/F1 fatless mice. The bone  $\mu$ CT values, including bone surface/bone volume (BS/BV) and trabecular spacing (Tb.Sp.), were significantly decreased, while trabecular number (Tb.N) was significantly increased in A-ZIP/F1 mice. The bone/tissue volume (BV/TV) ratio also indicated a higher trend ( $0.05 < p < .10$ ) in A-ZIP/F1 mice ( $n = 5$ ) compared with wild-type mice ( $n = 6$ ). Data are expressed as means  $\pm$  SD. Abbreviations: BMC, bone mineral content; BMD, bone mineral density; BS, bone surface; BV, bone volume; DMSO, dimethyl sulfoxide; Tb.N., Trabecular number; Tb.Sp., trabecular spacing; TV, tissue volume; WT, wild type.

### Osteoblast-Targeted PPAR $\gamma$ Knockout Increases Trabecular Number in Adult Mice

To directly assess bone mass when PPAR $\gamma$  is not expressed in osteoblasts, an inducible osteoblast-targeted PPAR $\gamma$  knockout mouse model was developed. Femurs from control and

experimental groups were harvested and analyzed at 6 months of age. Quantitative data from  $\mu$ CT analyses demonstrated that PPAR $\gamma$  deletion in osteoblasts had little effect on cortical bone as they demonstrated similar mean thickness and marrow area (Fig. 4A, 4B). In contrast, the structure of trabecular

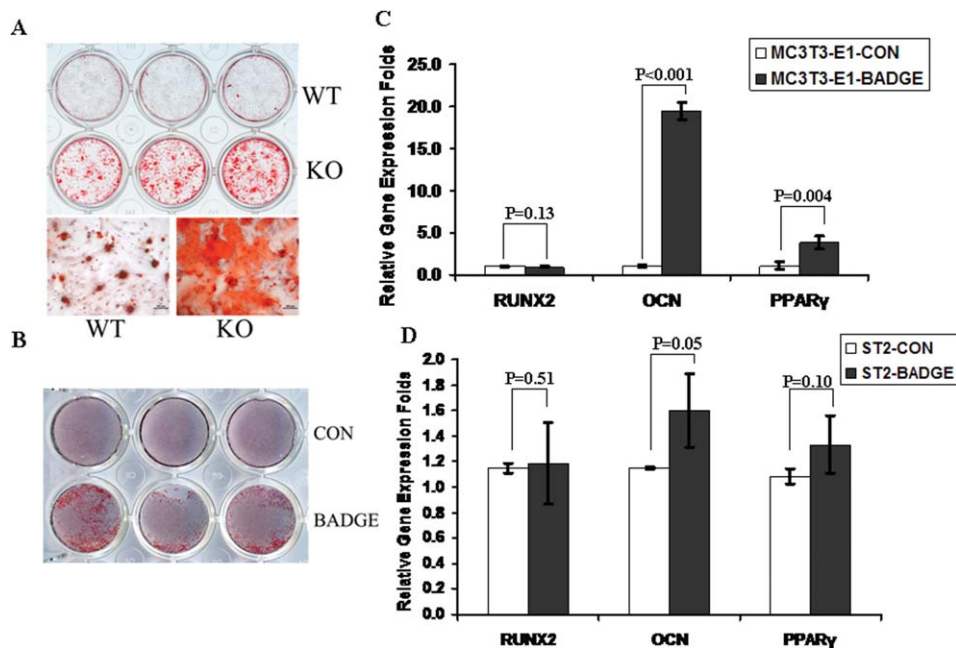


**Figure 3.** Osteoblast-targeted PPAR $\gamma$  suppression increased osteogenesis in vitro. (A): Osteoblast-targeted PPAR $\gamma$  knockout increases mineralization. Compared with the bone marrow mesenchymal stem cells (BMSCs) from WT mice, BMSCs from osteoblast-targeted PPAR $\gamma$  knockout mice demonstrated much higher mineralization after 2 week-culture in osteogenic differentiation medium ( $n = 3$ ). Scale bar = 100  $\mu$ m. (B): Mineralization is increased by PPAR $\gamma$  antagonist. The mineralization in MC3T3-E1 cells was enhanced when PPAR $\gamma$  was blocked by bisphenol A diglycidyl ether (BADGE) ( $n = 3$ ). (C, D) Gene expression in BADGE-treated ST2 and MC3T3-E1 cells. The effects of PPAR $\gamma$  inhibition on osteoblast-related gene expression in ST2 and MC3T3-E1 were tested after 24 hours BADGE treatment. Osteocalcin (OCN) gene expression was enhanced by BADGE, while no significant difference was noticed for Runx2 expression in either cell type. Expression of PPAR $\gamma$  was also slightly increased by BADGE treatment ( $n = 3$ ). Data are expressed as means  $\pm$  SD. Abbreviations: BADGE, bisphenol A diglycidyl ether; CON, control; KO, knockout; WT, wild type.

bone was significantly altered by deletion of *PPAR $\gamma$*  in osteoblasts (Fig. 4A, 4C). Among the trabecular analyses, trabecular number (Tb.N.) was significantly increased and trabecular spacing (Tb.Sp) was significantly decreased in *PPAR $\gamma$*  KO mice. The bone volume fraction (BV/TV) also indicated a clear trend towards increasing BV/TV ( $0.05 < p < .10$ ) in KO mice (Fig. 4A, 4C). Therefore, conditional deletion of *PPAR $\gamma$*  in osteoblasts significantly increased trabecular number, while it had limited effects on cortical bone. These in vivo data also suggest that *PPAR $\gamma$*  plays a direct role in osteoblastogenesis in addition to its primary role in adipogenesis.

### Suppression of Endogenous PPAR $\gamma$ Increases mTOR Signaling and Osteogenesis

The in vitro deletion of PPAR $\gamma$  in BMSCs dramatically elevated phosphorylation of p70S6K (p-p70S6K), which is the primary down-stream effector of mTOR signaling (Fig. 5A). Consistent with the increase in p-p70S6K, phosphorylation of AKT (p-AKT), which is one of the up-stream activators for mTOR signaling, was also enhanced when Ad-Cre was used to knockdown PPAR $\gamma$  (Fig. 5A). In complementary studies, the level of p-p70S6K was significantly increased in MC3T3-E1 and ST2 cells after 24-hour treatment with BADGE. It was noted that the basal level of p-p70S6K in ST2 cells was much lower than in 3T3-E1 cells. The levels of p-AKT were also increased in both cell types after BADGE-induced PPAR $\gamma$  suppression. In addition, treatment with BADGE resulted in elevated levels of Runx2 and/or OCN in ST2 and MC3T3-E1 cells (Fig. 5B). Consistent with the data supporting the hypothesis that PPAR $\gamma$  influences osteoblast differentiation by inhibiting mTOR signaling, mineralization of MC3T3-E1 cells exposed to BADGE was severely inhibited

by rapamycin treatment (Fig. 5C), suggesting that rapamycin can rescue the loss of PPAR $\gamma$  activity. These data indicate that endogenous PPAR $\gamma$  in osteoblasts inhibited the activity of mTOR signaling, which is essential for osteogenesis. Consistent with the in vitro data, the levels of phosphorylation of p70S6K (p-p70S6K, red staining) in osteoblasts and osteocytes were clearly increased in the PPAR $\gamma$  KO mice (Supporting Information Fig. 1). Therefore, our data strongly suggest that the negative effects of PPAR $\gamma$  on osteogenesis are partially mediated through inhibition of mTOR signaling.

## DISCUSSION

In the current study, PPAR $\gamma$  was specifically deleted in vitro and in osteoblasts in adult mice. Collectively, the data indicated that PPAR $\gamma$  negatively regulates osteoblast differentiation and bone formation. Additionally, it was determined that PPAR $\gamma$  inhibits mTOR signaling because either disruption of PPAR $\gamma$  expression, or treatment with the PPAR $\gamma$  inhibitor BADGE increases mTOR signaling and increases osteoblast differentiation.

In addition to adipogenesis, PPAR $\gamma$  regulates a variety of physiologic processes including lipid metabolism, insulin sensitivity, inflammation, angiogenesis and osteoclastogenesis [3,41–43]. Among these PPAR $\gamma$ -mediated physiologic processes, adipogenesis, inflammation, angiogenesis and osteoclastogenesis are known to be involved in bone homeostasis [3,41,44–46]. However, due to overlapping signaling in these complex biologic functions, it is difficult to distinguish the direct role and mechanism of action for PPAR $\gamma$  in osteogenesis [6,47,48]. Most of the available evidence suggests that the

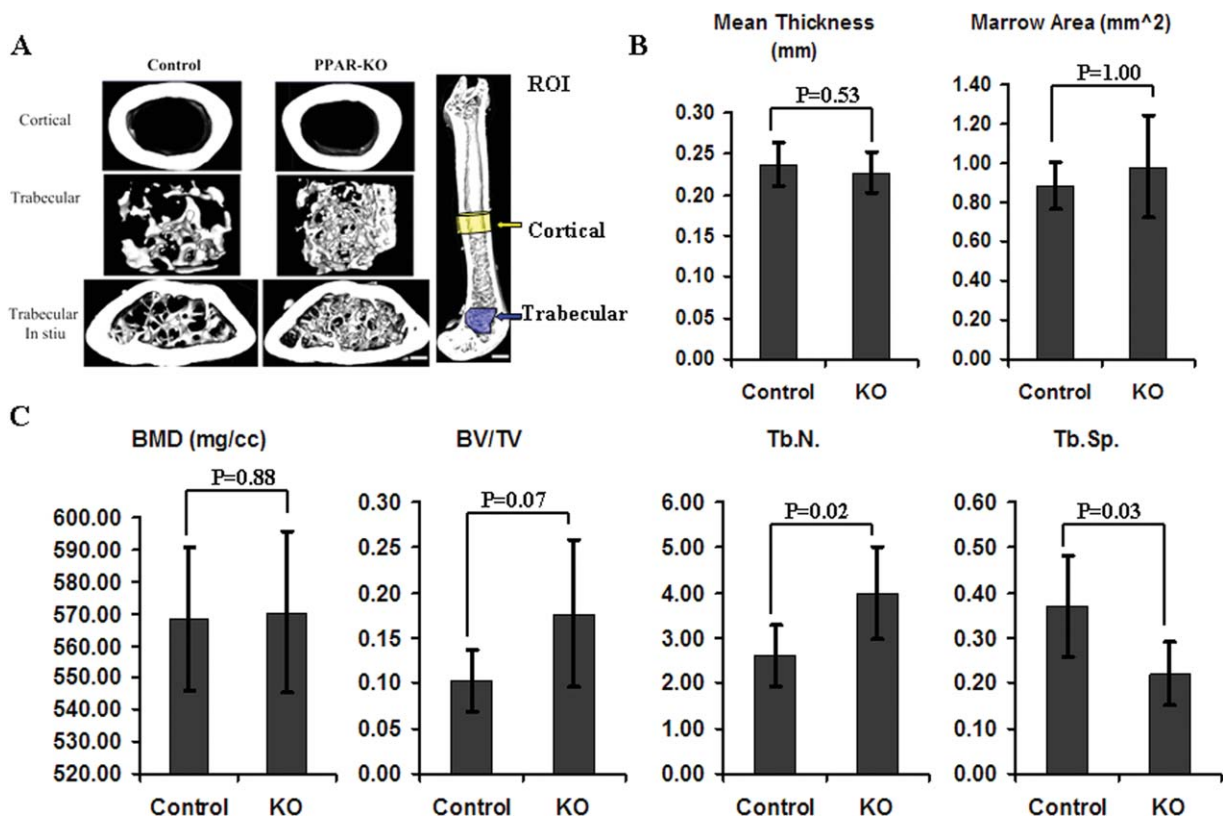


**Figure 4.** Osteoblast-Targeted PPAR $\gamma$  knockout increases trabecular number in adult mice. (A): 3D reconstructed  $\mu$ CT images of cortical, trabecular bone and the region of interest (ROI) for cortical and trabecular bone analyses in Control ( $n = 6$ ) and PPAR $\gamma$  KO group ( $n = 5$ ). Scale bar (left panel) = 250  $\mu$ m; Scale bar (right panel) = 1 mm. (B):  $\mu$ CT analysis of cortical bone. PPAR $\gamma$  deletion in osteoblasts had little effect on cortical bone as they demonstrated similar mean thickness and marrow area. (C):  $\mu$ CT analysis of trabecular bone. The structure of trabecular bone was significantly altered by deletion of PPAR $\gamma$  in osteoblasts. Trabecular number (Tb.N.) was significantly increased and trabecular spacing (Tb.Sp.) was significantly decreased in PPAR $\gamma$  KO mice. The bone volume fraction (BV/TV) also indicated a clear trend of increasing BV/TV ( $0.05 < p < .10$ ) in KO mice. Data are expressed as means  $\pm$  SD. Abbreviations: BMD, bone mineral density; BV, bone volume; KO, knockout; Tb.N., Trabecular number; Tb.Sp., trabecular spacing.

negative effects of PPAR $\gamma$  on bone formation are through an adipogenesis-dependent mechanism. This conclusion may be explained by the reciprocal relationship between osteoblasts and adipocytes, which are both derived from mesenchymal stem cells [49]. Furthermore, TZD treatment is known to stimulate the secretion of adiponectin and tumor necrosis factor alpha (TNF- $\alpha$ ) from fat tissue and thereby induce bone loss [50,51]. However, the notion of a reciprocal relationship between adipogenesis and osteogenesis in the marrow is challenged by emerging data that suggest that the inhibition of adipogenesis is not always accompanied by increased osteogenesis [16,17]. For example, systemic treatment with BADGE, a PPAR $\gamma$  antagonist, effectively blocks type I diabetes-induced hyperlipidemia and bone marrow adiposity. However, BADGE treatment is not able to block type I diabetes-induced bone loss [16]. In line with this *in vivo* finding, BADGE and GW9662, two antagonists of PPAR $\gamma$ , as well as lentivirus-mediated knockdown of PPAR $\gamma$ , inhibit adipocyte differentiation from MSC without significantly affecting osteogenesis [17].

Because of conflicting evidence linking adipogenesis and osteogenesis, we sought to directly study the contribution of PPAR $\gamma$  in osteogenic differentiation. We isolated BMSCs from PPAR $\gamma$  flox/flox mice and administered Ad-Cre to knockout PPAR $\gamma$  *in vitro*. Before cell harvest and addition of Ad-Cre, the flox/flox mice have the same phenotype as wild-type mice. Use of this system eliminates the potential for

systemic regulation of precursor cells that may otherwise be present in traditional phenotypically altered PPAR $\gamma$  knockout animals. Moreover, compared with the chemical antagonists (BADGE and GW9662), the Ad-Cre assay has minimal side effects because it is designed to specifically target the PPAR $\gamma$  gene. The *in vitro* data support the finding that PPAR $\gamma$  is essential for adipogenesis and that osteogenic differentiation is enhanced when endogenous PPAR $\gamma$  is deleted in BMSCs.

To further determine the effects of adipogenesis on bone formation, we used the A-ZIP/F1 mouse model. Adipogenesis in these mice is largely blocked due to the expression of a dominant-negative form of C/EBP under the adipocyte fatty-acid-binding protein four (FABP4) promoter, while the expression of PPAR $\gamma$  is not affected [39]. The  $\mu$ CT data demonstrated that both cortical and trabecular bone were significantly increased in these adipotrophic mice. In contrast, when adipogenesis was induced by PPAR $\gamma$  activation, osteogenesis was blocked in ST2 cells. It has also been reported that inhibition of adipogenesis in whole animals has profound effects in addition to regulation of osteogenesis. For example, in lipotrophic A-ZIP/F1 ‘fatless’ mice, and in mice treated with BADGE, marrow engraftment after irradiation is accelerated relative to wild-type or untreated mice [52]. This finding suggests that suppression of adipogenesis may not only enhance osteogenesis but may increase hematopoiesis as well.

In addition to the indirect adipogenesis-mediated effects of PPAR $\gamma$  on osteogenesis, several lines of study from *in vitro*



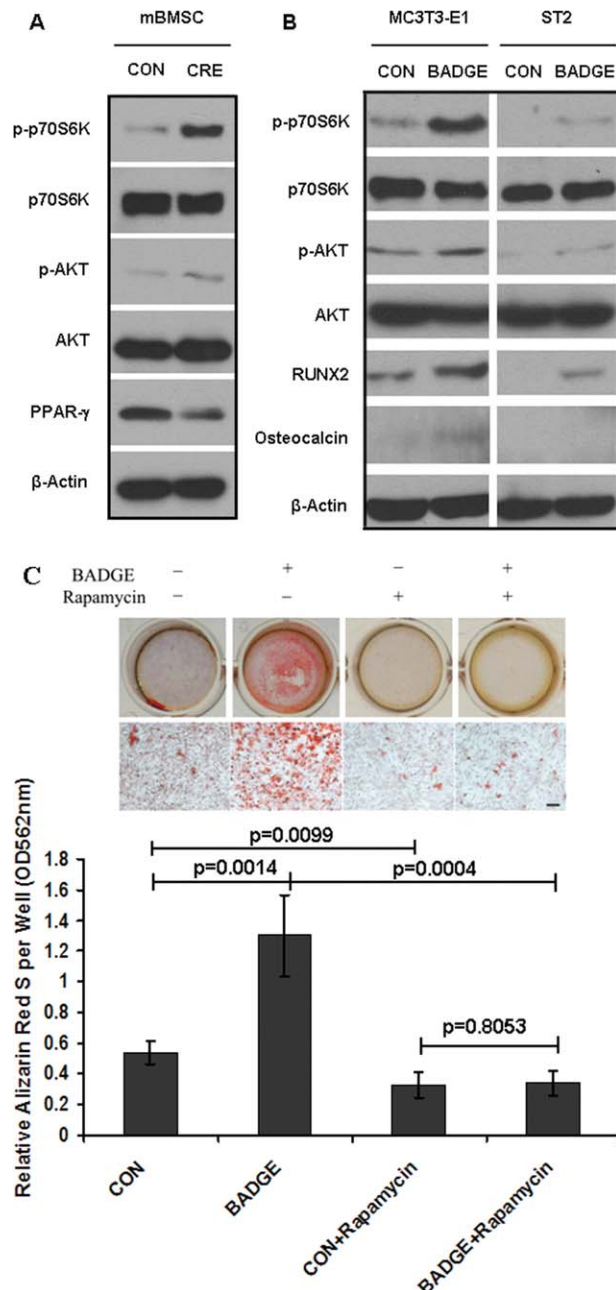


**Figure 5.** Suppression of endogenous PPAR $\gamma$  increases mTOR signaling and osteogenesis. (A): Deletion of PPAR $\gamma$  in bone marrow mesenchymal stem cells (BMSCs) dramatically increases mTOR signaling. Deletion of PPAR $\gamma$  in BMSCs dramatically elevated the phosphorylation of p70S6K (p-p70S6K) and phosphorylation of AKT (p-AKT). (B): Suppression of endogenous PPAR $\gamma$  by bisphenol A diglycidyl ether (BADGE) dramatically increases mTOR signaling in MC3T3-E1 and ST2 cells. The levels of p-AKT and p-p70S6K were increased in both cell types after BADGE-induced PPAR $\gamma$  suppression. BADGE-treatment resulted in the elevated levels of Runx2 and/or OCN in ST2 and MC3T3-E1 cells. (C): Rapamycin inhibits mineralization in osteoblasts. The BADGE-enhanced mineralization in MC3T3-E1 cells was severely inhibited by rapamycin-treatment ( $n = 3$ ). Data are expressed as means  $\pm$  SD. Abbreviations: BADGE, bisphenol A diglycidyl ether; CON, control; CRE, AdCRE group; mBMSC, bone marrow mesenchymal stem cell.

systems also suggest that PPAR $\gamma$  may have a direct effect on osteoblast differentiation. It has been reported by several groups that functional PPAR $\gamma$  is expressed in osteoblasts [11–13].

Moreover, the pro-adipogenic and anti-osteoblastic PPAR $\gamma$  activities can be separately activated by different ligands [53]. Further studies indicate that PPAR $\gamma$  pro-adipogenic activity involves binding to peroxisome proliferator-activated receptor-response element (PPRE) in gene regulatory regions while its anti-osteoblastic activity is PPRE-independent [54]. To study the role of PPAR $\gamma$  in osteoblast function, we specifically deleted PPAR $\gamma$  in osteoblasts by using the Cre/loxP system. BMSCs from the PPAR $\gamma$  KO (*Osx Cre/flox-PPAR $\gamma$* ) mice demonstrated a higher mineralization capacity compared with the cells from WT mice. Consistent with the *in vitro* results, the  $\mu$ CT analyses revealed that several trabecular bone parameters were significantly increased in PPAR $\gamma$  KO mice compared with the WT mice. Our findings are supported by a recent report that *in vivo* over-expression of PPAR $\gamma$  specifically in osteoblasts under the control of a 2.3-kb procollagen type 1 promoter negatively regulates bone mass in male mice [14]. It is noted that the over-expression model may result in more unexpected changes to the mice compared with our conditional KO model. Indeed, they disclose that osteoclastogenesis is significantly inhibited in mice overexpressing PPAR $\gamma$  [14]. However, it is known that PPAR $\gamma$  is a pro-osteoclastogenic regulator *in vitro* and *in vivo* [45]. Moreover, over-expression of PPAR $\gamma$  in osteoblasts unexpectedly increases adipogenesis of BMSCs *in vitro* although no significant difference *in vivo* was reported [14]. These drawbacks from the over-expression strategy are mitigated in the tetracycline (tet)-inducible Cre/loxP system (Tet-Off) used in our experiments. Tetracycline has been widely used in bone histomorphometry to label new bone formation [55] and to regulate the Cre recombinase gene in knockout mice [56]. Doxycycline, a member of the tetracycline family, was used in our control group to maintain normal PPAR $\gamma$  functions by inhibiting the expression of Cre recombinase. However, it has been reported that tetracyclines are able to increase bone formation by both increasing osteoblast activity and inhibiting osteoclast function [57]. Therefore, the difference in bone formation due to PPAR $\gamma$  knockout may be masked by doxycycline treatment, which is one of the possible reasons that BVF ( $p = 0.07$ ) did not achieve statistical significance in the KO group relative to the control group, because our control group was provided doxycycline to repress Cre activity.

Our data indicate that PPAR $\gamma$  is able to regulate osteoblast differentiation and bone formation through both indirect and direct mechanisms. The indirect pathway is related to reciprocal differentiation as has been discussed previously.

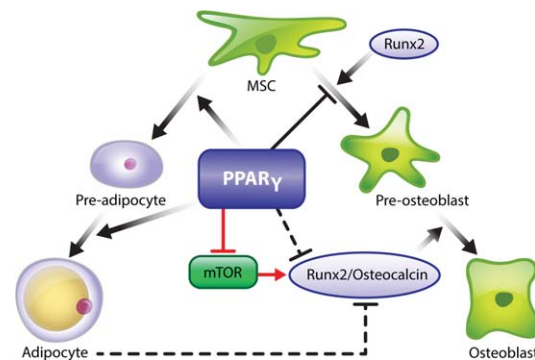


**Figure 6.** PPAR $\gamma$  modulates bone formation through direct and indirect mechanisms. The indirect pathway is dependent on adipogenesis, which includes not only the role of PPAR $\gamma$  in the allocation of stem cells, but also the potential negative regulation derived from adipocytes. The direct mechanism is independent on adipogenesis. The endogenous PPAR $\gamma$  in osteoblasts strongly inhibits the mTOR activity, thus inhibiting Runx2/Osteocalcin mediated osteoblastic differentiation. Abbreviations: MSC, mesenchymal stem cell; mTOR, mammalian target of rapamycin.

The direct regulation of osteogenesis, however, is not completely defined. Our recent work indicates that mTOR is directly involved in odontoblast and osteoblast differentiation [26,27]. The contribution of mTOR to bone formation is further confirmed by a recent study in which significantly less bone formation and a lower trabecular bone mass was observed in rapamycin-treated C57BL/6 mice compared with the vehicle-treated controls [31]. It is intriguing that in the current study we demonstrated that the Akt/mTOR/p70S6K pathway was activated after knockout of PPAR $\gamma$  in BMSCs, or by a PPAR $\gamma$  antagonist in osteoblasts. Accordingly, osteoblastic markers were increased by the suppression of PPAR $\gamma$  activity. Moreover, osteoblastic differentiation following the suppression of PPAR $\gamma$  was blocked by rapamycin. Our data are consistent with the previous finding that rapamycin inhibits osteoblast differentiation, while over-expression of p70S6K significantly increases levels of Runx2 protein and Runx2 activity [29]. These results clearly indicate that the mTOR pathway is essential for osteoblast differentiation and that it is largely inhibited by endogenous PPAR $\gamma$  in osteoblasts.

### SUMMARY

In summary, our data demonstrate that PPAR $\gamma$  modulates bone formation through bimodal mechanisms (Fig. 6). The

indirect pathway is dependent on adipogenesis, which includes not only the role of PPAR $\gamma$  in the commitment of stem cells, but also the potential for negative regulation by adjacent mature adipocytes. The direct mechanism is independent of adipogenesis. The direct suppression of PPAR $\gamma$  in osteoblasts significantly increases osteoblast differentiation and trabecular bone formation which is demonstrated in the Osx-PPAR $\gamma$  knockout mouse model. We further demonstrate that endogenous PPAR $\gamma$  in osteoblasts strongly inhibits mTOR activity, thus inhibiting osteoblastic differentiation.

### ACKNOWLEDGMENTS

This study was supported by NIH grants R01-AR-054714 (to K.D.H.) and R01-DK-082481 (to P.H.K.). We thank Dr. Erica L. Scheller for helpful discussions and comments on the manuscript and Derek Dopkin and Jason Combs for outstanding technical assistance.

### DISCLOSURE OF POTENTIAL CONFLICTS OF INTEREST

The authors declare no potential conflicts of interest.

### REFERENCES

- Rosen ED, Sarraf P, Troy AE, Bradwin G, Moore K, Milstone DS, Spiegelman BM, Mortensen RM. PPAR $\gamma$  is required for the differentiation of adipose tissue in vivo and in vitro. *Mol Cell* 1999;4:611–617.
- Tontonoz P, Hu E, Spiegelman BM. Stimulation of adipogenesis in fibroblasts by PPAR $\gamma$ 2, a lipid-activated transcription factor. *Cell* 1994;79:1147–1156.
- Tontonoz P, Spiegelman BM. Fat and beyond: The diverse biology of PPAR $\gamma$ . *Ann Rev Biochem* 2008;77:289–312.
- Betteridge DJ. Thiazolidinediones and fracture risk in patients with type 2 diabetes. *Diab Med* 2011;28:759–771.
- Meunier P, Aaron J, Edouard C, Vignon G. Osteoporosis and the replacement of cell populations of the marrow by adipose tissue: A quantitative study of 84 iliac bone biopsies. *Clin Orthopaed Relat Res* 1971;80:147–154.
- Akune T, Ohba S, Kamekura S, Yamaguchi M, Chung U-i, Kubota N, Terauchi Y, Harada Y, Azuma Y, Nakamura K, Kadowaki T, Kawaguchi H. PPAR  $\gamma$  insufficiency enhances osteogenesis through osteoblast formation from bone marrow progenitors. *J Clin Invest* 2004;113:846–855.
- Liu L-F, Shen W-J, Zhang ZH, Wang LJ, Kraemer FB. Adipocytes decrease Runx2 expression in osteoblastic cells: Roles of PPAR $\gamma$  and adiponectin. *J Cell Physiol* 2010;225:837–845.
- Shinoda Y, Yamaguchi M, Ogata N, Akune T, Kubota N, Yamauchi T, Terauchi Y, Kadowaki T, Takeuchi Y, Fukumoto S, Ikeda T, Hoshi K, Chung U-i, Nakamura K, Kawaguchi H. Regulation of bone formation by adiponectin through autocrine/paracrine and endocrine pathways. *J Cell Biochem* 2006;99:196–208.
- Scheller EL, Song J, Dishowitz MI, Soki FN, Hankenson KD, Krebsbach PH. Leptin functions peripherally to regulate differentiation of mesenchymal progenitor cells. *Stem Cells* 2010;28:1071–1080.
- Ducy P, Amling M, Takeda S, Priemel M, Schilling AF, Beil FT, Shen J, Vinson C, Rueger JM, Karsenty G. Leptin inhibits bone formation through a hypothalamic relay: A central control of bone mass. *Cell* 2000;100:197–207.
- Mbalaviele G, Abu-Amer Y, Meng A, Jaiswal R, Beck S, Pittenger MF, Thiede MA, Marshak DR. Activation of peroxisome proliferator-activated receptor- $\gamma$  pathway inhibits osteoclast differentiation. *J Biological Chem* 2000;275:14388–14393.
- Maurin AC, Chavassieux PM, Meunier PJ. Expression of PPAR $\gamma$  and  $\beta/\delta$  in human primary osteoblastic cells: Influence of polyunsaturated fatty acids. *Calc Tissue Int* 2005;76:385–392.
- Jackson SM, Demer LL. Peroxisome proliferator-activated receptor activators modulate the osteoblastic maturation of MC3T3-E1 preosteoblasts. *FEBS Lett* 2000;471:119–124.
- Cho SW, Yang J-Y, Her SJ, Choi HJ, Jung JY, Sun HJ, An JH, Cho HY, Kim SW, Park KS, Kim SY, Baek W-Y, Kim J-E, Yim M, Shin CS. Osteoblast-targeted overexpression of PPAR $\gamma$  inhibited bone mass gain in male mice and accelerated ovariectomy-induced bone loss in female mice. *J Bone Mineral Res* 2011;26:1939–1952.
- Kim SW, Her SJ, Kim SY, Shin CS. Ectopic overexpression of adipogenic transcription factors induces transdifferentiation of MC3T3-E1 osteoblasts. *Biochem Biophys Res Commun* 2005;327:811–819.
- Botolin S, McCabe LR. Inhibition of PPAR $\gamma$  prevents type I diabetic bone marrow adiposity but not bone loss. *J Cell Physiol* 2006;209:967–976.
- Yu W-H, Li F-G, Chen X-Y, Li J-T, Wu Y-H, Huang L-H, Wang Z, Li P, Wang T, Lahn BT, Xiang AP. PPAR $\gamma$  suppression inhibits adipogenesis but does not promote osteogenesis of human mesenchymal stem cells. *Int J Biochem Cell Biol* 2011;44:377–384.
- Zoncu R, Efeyan A, Sabatini DM. mTOR: From growth signal integration to cancer, diabetes and ageing. *Nat Rev Mol Cell Biol* 2011;12:21–35.
- Akiyama TE, Sakai S, Lambert G, Nicol CJ, Matsusue K, Pimprale S, Lee Y-H, Ricote M, Glass CK, Brewer HB, Gonzalez FJ. Conditional disruption of the peroxisome proliferator-activated receptor gamma gene in mice results in lowered expression of ABCA1, ABCG1, and ApoE in macrophages and reduced cholesterol efflux. *Mol Cell Biol* 2002;22:2607–2619.
- Nojima H, Tokunaga C, Eguchi S, Oshiro N, Hidayat S, Yoshino K-i, Hara K, Tanaka N, Avruch J, Yonezawa K. The mammalian target of rapamycin (mTOR) partner, raptor, binds the mtor substrates p70 S6 kinase and 4E-BP1 through their Tor signaling (Tos) motif. *J Biological Chem* 2003;278:15461–15464.
- Jacinto E, Loewith R, Schmidt A, Lin S, Ruegg MA, Hall A, Hall MN. Mammalian TOR complex 2 controls the actin cytoskeleton and is rapamycin insensitive. *Nat Cell Biol* 2004;6:1122–1128.
- SamPATH P, Pritchard DK, Pabon L, Reinecke H, Schwartz SM, Morris DR, Murry CE. A hierarchical network controls protein translation during murine embryonic stem cell self-renewal and differentiation. *Cell Stem Cell* 2008;2:448–460.
- Dunlop EA, Dodd KM, Seymour LA, Tee AR. Mammalian target of rapamycin complex 1-mediated phosphorylation of eukaryotic initiation factor 4E-binding protein 1 requires multiple protein-protein interactions for substrate recognition. *Cell Signal* 2009;21:1073–1084.
- Easley CA, Ben-Yehudah A, Redinger CJ, Oliver SL, Varum ST, Eisinger VM, Carlisle DL, Donovan PJ, Schatten GP. mTOR-mediated activation of p70 S6K induces differentiation of pluripotent human embryonic stem cells. *Cell Reprogram* 2010;12:263–73.

- 25 Turnquist HR, Cardinal J, Macedo C, Rosborough BR, Sumpter TL, Geller DA, Metes D, Thomson AW. mTOR and GSK-3 shape the CD4+ T-cell stimulatory and differentiation capacity of myeloid DCs after exposure to LPS. *Blood* 2010;115:4758–69.
- 26 Kim J, Jung Y, Sun H, Joseph J, Mishra A, Shiozawa Y, Wang J, Krebsbach PH, Taichman RS. Erythropoietin mediated bone formation is regulated by mTOR signaling. *J Cell Biochem* 2012;113:220–228.
- 27 Kim J-K, Baker J, Nor JE, Hill EE. mTor plays an important role in odontoblast differentiation. *J Endodont* 2011;37:1081–1085.
- 28 Tang C-H, Lu D-Y, Tan T-W, Fu W-M, Yang R-S. Ultrasound induces hypoxia-inducible factor-1 activation and inducible nitric-oxide synthase expression through the integrin/integrin-linked kinase/Akt/mammalian target of rapamycin pathway in osteoblasts. *J Biological Chem* 2007;282:25406–25415.
- 29 Singha UK, Jiang Y, Yu S, Luo M, Lu Y, Zhang J, Xiao G. Rapamycin inhibits osteoblast proliferation and differentiation in MC3T3-E1 cells and primary mouse bone marrow stromal cells. *J Cell Biochem* 2008;103:434–446.
- 30 Tseng W-P, Yang S-N, Lai C-H, Tang C-H. Hypoxia induces BMP-2 expression via ILK, Akt, mTOR, and HIF-1 pathways in osteoblasts. *J Cell Physiol* 2010;223:810–818.
- 31 Xian L, Wu X, Pang L, Lou M, Rosen CJ, Qiu T, Crane J, Frassica F, Zhang L, Rodriguez JP, Jia X, Yakar S, Xuan S, Efstratiadis A, Wan M, Cao X. Matrix IGF-1 maintains bone mass by activation of mTOR in mesenchymal stem cells. *Nat Med* 2012;18:1095–1101.
- 32 Laplante M, Sabatini DM. An emerging role of Mtor in lipid biosynthesis. *Curr Biol* 2009;19:R1046–R1052.
- 33 Kim JE, Chen J. Regulation of peroxisome proliferator-activated receptor- $\gamma$  activity by mammalian target of rapamycin and amino acids in adipogenesis. *Diabetes* 2004;53:2748–2756.
- 34 Krebsbach PH, Kuznetsov SA, Satomura K, Emmons RVB, Rowe DW, Robey PG. Bone formation in vivo: Comparison of osteogenesis by transplanted mouse and human marrow stromal fibroblasts. *Transplantation* 1997;63:1059–1069.
- 35 Sun H, Dai K, Tang T, Zhang X. Regulation of osteoblast differentiation by Slit2 in osteoblastic cells. *Cell Tissue Organ* 2009;190:69–80.
- 36 Bennett CN, Longo KA, Wright WS, Suva LJ, Lane TF, Hankenson KD, MacDougald OA. Regulation of osteoblastogenesis and bone mass by Wnt10b. *Proc Natl Acad Sci U S A* 2005;102:3324–3329.
- 37 Nicol CJ, Yoon M, Ward JM, Yamashita M, Fukamachi K, Peters JM, Gonzalez FJ. PPAR $\gamma$  influences susceptibility to DMBA-induced mammary, ovarian and skin carcinogenesis. *Carcinogenesis* 2004;25:1747–1755.
- 38 Rodda SJ, McMahon AP. Distinct roles for hedgehog and canonical Wnt signaling in specification, differentiation and maintenance of osteoblast progenitors. *Development* 2006;133:3231–3244.
- 39 Moitra J, Mason MM, Olive M, Krylov D, Gavrilova O, Marcus-Samuels B, Feigenbaum L, Lee E, Aoyama T, Eckhaus M, Reitman ML, Vinson C. Life without white fat: A transgenic mouse. *Genes Dev* 1998;12:3168–81.
- 40 Bouxsein ML, Boyd SK, Christiansen BA, Guldberg RE, Jepsen KJ, Müller R. Guidelines for assessment of bone microstructure in rodents using micro-computed tomography. *J Bone Mineral Res* 2010;25:1468–1486.
- 41 Wan YH. PPAR gamma in bone homeostasis. *Trends Endocrinol Metabol* 2010;21:722–728.
- 42 Lecka-Czernik B. PPAR[gamma], an essential regulator of bone mass: Metabolic and molecular cues. *IBMS Bonekey* 2010;7:171–181.
- 43 Magri CJ, Gatt N, Xuereb RG, Fava S. Peroxisome proliferator-activated receptor- $\gamma$  and the endothelium: Implications in cardiovascular disease. *Expert Rev Cardiovasc Ther* 2011;9:1279–1294.
- 44 Devlin MJ, Kawai M, Rosen CJ. Fat targets for skeletal health. *Nature Rev Rheumatol* 2009;5:365.
- 45 Wan Y, Chong L-W, Evans RM. PPAR-[gamma] regulates osteoclastogenesis in mice. *Nat Med* 2007;13:1496–1503.
- 46 Gerber H-P, Ferrara N. Angiogenesis and bone growth. *Trends Cardiovasc Med* 2000;10:223–228.
- 47 Rzonca SO, Suva LJ, Gaddy D, Montague DC, Lecka-Czernik B. Bone is a target for the antidiabetic compound rosiglitazone. *Endocrinology* 2004;145:401–406.
- 48 Ali AA, Weinstein RS, Stewart SA, Parfitt AM, Manolagas SC, Jilka RL. Rosiglitazone causes bone loss in mice by suppressing osteoblast differentiation and bone formation. *Endocrinology* 2005;146:1226–1235.
- 49 Pittenger MF, Mackay AM, Beck SC, Jaiswal RK, Douglas R, Mosca JD, Moorman MA, Simonetti DW, Craig S, Marshak DR. Multilineage potential of adult human mesenchymal stem cells. *Science* 1999;284:143–147.
- 50 Halade GV, El Jamali A, Williams PJ, Fajardo RJ, Fernandes G. Obesity-mediated inflammatory microenvironment stimulates osteoclastogenesis and bone loss in mice. *Exp Gerontol* 2011;46:43–52.
- 51 Luo X-H, Guo L-J, Xie H, Yuan L-Q, Wu X-P, Zhou H-D, Liao E-Y. Adiponectin Stimulates RANKL and inhibits OPG expression in human osteoblasts through the MAPK signaling pathway. *J Bone Mineral Res* 2006;21:1648–1656.
- 52 Naveiras O, Nardi V, Wenzel PL, Hauschka PV, Fahey F, Daley GQ. Bone-marrow adipocytes as negative regulators of the haematopoietic microenvironment. *Nature* 2009;460:259–263.
- 53 Lecka-Czernik B, Moerman EJ, Grant DF, Lehmann JM, Manolagas SC, Jilka RL. Divergent effects of selective peroxisome proliferator-activated receptor- $\gamma$ 2 ligands on adipocyte versus osteoblast differentiation. *Endocrinology* 2002;143:2376–2384.
- 54 Shockley KR, Lazarenko OP, Czernik PJ, Rosen CJ, Churchill GA, Lecka-Czernik B. PPAR $\gamma$ 2 nuclear receptor controls multiple regulatory pathways of osteoblast differentiation from marrow mesenchymal stem cells. *J Cell Biochem* 2009;106:232–246.
- 55 Frost HM. Tetracycline-based histological analysis of bone remodeling. *Calcified Tissue Res* 1969;3:211.
- 56 Branda CS, Dymecki SM. Talking about a revolution: The impact of site-specific recombinases on genetic analyses in mice developmental. *Cell* 2004;6:7–28.
- 57 Payne JB, Golub LM. Using tetracyclines to treat osteoporotic/osteopenic bone loss: From the basic science laboratory to the clinic. *Pharmacological research*. 2011;63:121–129.



See [www.StemCells.com](http://www.StemCells.com) for supporting information available online.